



A model to analyse anisotropic magnetoresistance

ÖMER F BAKKALOĞLU

Department of Engineering Physics, Faculty of Engineering, Gaziantep University,
27310 Şehitkamil, Gaziantep, Turkey
E-mails: bakkaloglu@gantep.edu.tr; ofb961@gmail.com

MS received 19 July 2020; revised 23 October 2021; accepted 2 December 2021

Abstract. In this study, an attempt is made to develop a model to analyse the anisotropic magnetoresistance in ferromagnetic metal films. In the model, the change in resistivity due to the changes in the scattering processes of the conduction electrons on applying an external magnetic field is proposed to be proportional to the spin-orbit interaction energy $\Delta U_{\text{SOI}} = \mu_0 \mu M/2$. Expressions are developed which relate the resistivity of the sample under an applied external magnetic field to its initial resistivity, current density, conduction electron magnetic moment, sample length, saturation magnetisation, remanence magnetisation, coercive field and external magnetic field. The equations obtained agree well with the experimental anisotropic magnetoresistance data of the ferromagnetic films.

Keywords. Anisotropic magnetoresistance; ferromagnetic materials; alloys; thin films.

PACS Nos 72.15.Gd; 75.47.-m; 75.50.-Ss; 75.70.-i

1. Introduction

Magnetic materials which can be influenced by the application of magnetic fields are a challenging area for scientists interested in the basics of magnetism and its applications. The application of a magnetic field influences the translational and rotational motions of a particle that has a magnetic moment and may therefore cause changes in electrical resistance, fluid flow, concentration, convection and other parameters in a magnetic system [1–28]. In magnetic recording technology, the change in electrical resistivity (and therefore resistance) in a magnetic metal under the influence of an applied magnetic field is widely used for developing read/write heads. The resistivity of a ferromagnetic metal is generally affected by the presence of phonons, impurities and magnetic entities within the material [23]. In this article, we study the influence of the magnetic field on the flow (motion) of conduction electrons in a ferromagnetic metal, which may cause a change in the resistivity of the material. The change in resistivity of a magnetic metal under the influence of an applied magnetic field is defined as magnetoresistance (MR). There are several types of magnetoresistance effects such as anisotropic, giant, tunnelling, colossal magnetoresistance effects, etc. [5–9, 16–27].

Anisotropic magnetoresistance (AMR) is described as the dependency of the magnetoresistance effect on the orientation of electric current with respect to the applied external magnetic field [24]. When the measurement is done by applying an external magnetic field along the direction of the electric current (known as the longitudinal magnetoresistance (LMR) measurement), an increase in the resistivity of the ferromagnetic metal samples is observed. When the measurement is done by applying an external magnetic field perpendicular to the direction of the electric current (known as the transverse magnetoresistance (TMR) measurement), a decrease in the resistivity of ferromagnetic metal samples is observed [25]. In ferromagnetic metals, LMR is generally observed to be greater than TMR. When there is no applied external magnetic field, the initial (natural) resistivity of the ferromagnetic metal in its equilibrium state is determined by the intrinsic magnetic quantities. In its equilibrium state, the overall magnetisation of the ferromagnetic metal is zero. However, local magnetic moments contribute to the scattering process of conduction electrons and the resistivity of the metal includes this magnetic scattering contribution in addition to other non-magnetic scattering processes. AMR effects in ferromagnetic metals are due to the replacement of external magnetic field \mathbf{H} by an internal field \mathbf{B} proportional to the magnetisation \mathbf{M} [26].

The effect of an electron's orbital motion on the orientation of its spin is described as the spin-orbit interaction (SOI), which is used to explain the AMR effect in materials. The effect of spin on the electrical conduction in ferromagnetic metals was studied by Mott [27] and then experimentally observed in ferromagnetic metal alloys [28–30]. In theoretical studies of the AMR effect, a two-current model is generally used while the operative scattering mechanism is recognised to be the SOI [19,20,23,24,26–28,30]. Two examples of the models are the Campbell–Fert–Jaoul (CFJ) model and the Malozemoff extended CFJ model, which are applicable for ferromagnetic materials [19,20,22]. The expressions obtained in these theoretical studies are usually long and a bit complicated.

Therefore, the main aim of this study, using energy considerations is: (1) to obtain much simpler equations for LMR and TMR effects than those present in the literature to predict the shape of magnetoresistance curves, (2) to fit the experimental (LMR and TMR) data of any ferromagnetic materials (which obey the basic principles of conduction electron flow, magnetism and the SOI) and (3) to explain the difference between LMR and TMR using the model developed.

2. Model

The initial resistivity ρ_0 and initial electric current density J_0 of a metal are related by Ohm's law [26] to the initial applied voltage V_0 and the sample length x as

$$J_0\rho_0 = V_0/x. \quad (1)$$

For a constant value of J_0 and x , as ρ_0 changes to ρ , V_0 changes to V . However, the change in resistivity may contain the changes in both voltage V (or energy $U = qV$) and current density J . If both ρ_0 and J_0 do not remain constant and change to ρ and J respectively, V_0 changes to V . In this case, the changes in the current density and voltage (energy) must be proportionally different to obtain a change in resistivity (from $\rho_0 = V_0/J_0x$ to $\rho = V/Jx$).

Let ρ_0 increase to ρ and J_{0L} decrease to J_L on applying an external magnetic field on the ferromagnetic metal sample in the longitudinal MR geometry, which is carried out at a constant current density J_{0L} . When ρ_0 increases to ρ , J_{0L} should decrease to J_L (uncompensated current density) because of the increase in resistivity. Meanwhile, V_0 increases by a voltage of ΔV_j to maintain a constant current density J_{0L} . So, voltage V_0 changes to V to maintain constant current density J_{0L} (i.e., responding to the change in resistivity and the so-called attempted change in the current density (from J_{0L} to J_L)) and becomes $V = V_0 + \Delta V_j$. In a similar

treatment to the longitudinal MR geometry above, in the transverse MR measurement which is done at a constant current density J_{0T} with a resistivity decrease, when ρ_0 decreases to ρ , J_{0L} should increase to J_T (uncompensated current density) because of the decrease in the resistivity. Meanwhile, V_0 decreases by a voltage of ΔV_j to maintain constant current density J_{0T} (i.e., responding to the change in resistivity and the so-called attempted change in current density (from J_{0T} to J_T)) and becomes $V = V_0 - \Delta V_j$.

When we measure the percentage MR change as $MRR\% = (\rho - \rho_0)/\rho_0 = (V - V_0)/V_0$ with constant current, constant cross-sectional area and constant length of the sample in these experiments, the change in electric potential $(V - V_0)/V_0 = \pm\Delta V_j/V_0$ may contain the so-called attempted change in current density (J_0 to J) for any change in resistivity (ρ_0 to ρ).

2.1 Longitudinal magnetoresistance measurement in ferromagnetic metals

When an external magnetic field \mathbf{H} is applied parallel to the electric current I in the ferromagnetic metal, a net magnetisation \mathbf{M} develops within the ferromagnetic metal along the direction of electric current as shown in figure 1. The creation of net magnetisation \mathbf{M} is due to the orientation of the atomic magnetic moments towards the direction of the applied external magnetic field and the electric current.

According to the scattering mechanism, as the atom's magnetic moment, which is due to the spin motion of the d-electron in ferromagnetic transition metals, rotates towards the applied external magnetic field, the electron cloud about each nucleus rearranges (deforms) slightly due to the SOI [31]. In the LMR geometry, this rearrangement increases the amount of the projected cross-sectional area of the electron cloud of the atom facing the flow of the conduction electrons, which is where the conduction electrons interact in a scattering process.

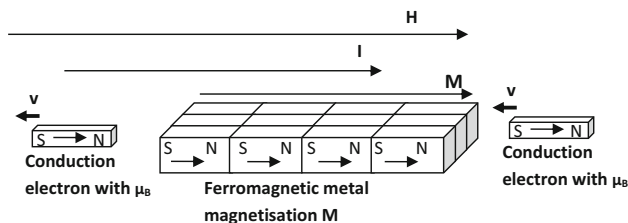


Figure 1. Motion of the conduction electron in the presence of magnetisation in the longitudinal MR measurement where \mathbf{H} is the applied external magnetic field, I is the applied electric current, v is the velocity, μ_B is the magnetic moment of the conduction electron and \mathbf{M} is the magnetisation of the sample.

Different values of this projected cross-sectional area for $\mathbf{H}=0$ or $\mathbf{H}\neq 0$ cause different amounts of scattering by the conduction electrons during their passage through the material. Thus, increased SOI is expected to cause more rearrangement of electron clouds and more conduction electron scattering. It may be logical to expect the change in the energy (or the decrease in the energy in this geometry) of a scattered conduction electron in this process to be proportional to the SOI energy.

The mechanism of this scattering process in transition metals is explained with Mott’s model [27]. According to this model, the hybridisation of s and d states brings the role of orbital angular momentum into the conduction process (therefore connecting magnetism with electrical transport properties). The SOI process causes the unsymmetrical mixture of spin-up and spin-down states, which eases the s–d transitions of the electrons. Empty d states can be occupied temporarily by conduction electrons, providing a spin-dependent and orbital angular momentum-dependent scattering process. However, s electrons can only scatter into the 3d hole states if the conduction electron momentum is in the plane of the classical orbit of the empty d state. When magnetisation \mathbf{M} is parallel to the current density J , a greater fraction of the empty 3d states becomes available. Therefore, new s–d scattering channels are more likely in the LMR geometry so that greater projected cross-sectional area, mentioned above, corresponds to greater magnetisation \mathbf{M} and a greater likelihood of having s–d scattering interaction in this geometry. By this mechanism, the microscopic internal field \mathbf{B} associated with \mathbf{M} couples to the current density via the SOI interactions between the trajectory (orbit) and magnetisation (spin) \mathbf{M} in ferromagnetic materials [26].

The energy involved in the SOI is given as $\Delta U_{\text{SOI}} = \mu B/2$ where $B = \mu_0 M$ [26]. In this expression, μ is the magnetic moment of the electron due to its spin motion (which involves the SOI with its trajectory (orbital) motion) and is taken to be equal to the Bohr magneton ($\mu_B = 9.274 \times 10^{-24}$ J/T), μ_0 is the magnetic permeability of free space which is equal to $4\pi \times 10^{-7}$ T·m/A.

The formation of net magnetisation in the LMR measurement increases the amount of s–d scattering interactions between the conduction electron and the atom. In this increased scattering interaction process, each conduction electron loses more energy (relative reduction in its initial energy) with respect to the case under the initial conditions before the application of the external magnetic field \mathbf{H} .

According to the model suggested in this study, the amount of energy lost by the conduction electrons in the scattering process in the sample compared with that under the initial conditions is proposed to be proportional to the SOI energy of $\Delta U_{\text{SOI}} = \mu_0 \mu M/2$.

The relative reduction in the energy of the conduction electrons is expected to give rise to a reduction in the current density as well. Eventually, an increase in the resistivity and therefore a change in the variable applied electric voltage occur to maintain a constant electric current as discussed above.

In other words, ρ_0 is the initial resistivity and J_{0L} is the initial current density in the ferromagnetic metal if an electric potential difference is applied before applying any external magnetic field. When an external magnetic field is applied along the direction of current on the ferromagnetic metal, the initial resistivity ρ_0 and the initial current density J_{0L} change to new values of ρ and J_L due to the decrease in the energy of conduction electrons in this scattering process. The relation between J_L and J_{0L} may be assumed to be $J_L = a_{JL} J_{0L}$ where a_{JL} relates J_{0L} to a smaller current density J_L .

The relation between ρ and ρ_0 can then be written by assuming the presence of these changes in both ρ_0 and J_{0L} as

$$\rho = \rho_0 + \Delta\rho, \tag{2}$$

where $\Delta\rho$ represents the increase in resistivity due to the decrease in energy of conduction electrons and the associated change (decrease) in current density from J_{0L} to J_L in the ferromagnetic metal, which can be obtained as follows:

Using Ohm’s law

$$\text{When } \mathbf{H}=0 \rightarrow R_0 = \rho_0 x/A = V_0/I_0$$

$$\text{When } \mathbf{H}\neq 0 \rightarrow R = \rho x/A = V/I.$$

The change in resistance is

$$\begin{aligned} \Delta R &= R - R_0 \rightarrow \rho x/A - \rho_0 x/A \\ &= (V/I) - (V_0/I_0) \rightarrow (\rho - \rho_0) \\ &= (V/xJ) - (V_0/xJ_0) \end{aligned}$$

with $J = I/A$ and $J_0 = I_0/A$.

Then using the relations $V = U/e$ and $V_0 = U_0/e$,

$$(\rho - \rho_0) = [(U/x e J) - (U_0/x e J_0)],$$

where e is the charge of the conduction electron, U and U_0 are the energies of conduction electron when $\mathbf{H}\neq 0$ and $\mathbf{H}=0$, respectively.

For the LMR measurement,

$$(\rho - \rho_0) = [(U_L/x e J_L) - (U_0/x e J_{0L})].$$

Using $J_L = a_{JL} J_{0L}$ and assuming $U_L = a_{uL} U_0$ where a_{uL} relates U_0 to a smaller energy U_L , then we can write

$$(\rho - \rho_0) = [(a_{uL} U_0/x e a_{JL} J_{0L}) - (U_0/x e J_{0L})],$$

$$(\rho - \rho_0) = [(a_{uL}/a_{JL}) - 1] U_0/x e J_{0L}$$

or

$$(\rho - \rho_0) = [(a_{uL} - a_{JL})/a_{JL}] U_0/x e J_{0L}.$$

For positive LMR, $a_{uL} > a_{jL} \rightarrow (a_{uL}/a_{jL}) > 1$, for negative LMR, $a_{uL} < a_{jL} \rightarrow (a_{uL}/a_{jL}) < 1$ and for zero LMR, $a_{uL} = a_{jL}$. This analysis shows that a greater difference between a_{uL} and a_{jL} causes a greater LMR effect.

Using $\Delta\rho = (\rho - \rho_0)$, it can be written as

$$\Delta\rho = \Delta U/(xeJ_L), \quad (3)$$

where $\Delta U = (a_{uL} - a_{jL})U_0$ with parameters a_{uL} and a_{jL} standing for the changes in the energy U_0 and the current density $J_L = a_{jL}J_{0L}$ respectively. In this study, ΔU is assumed to be proportional to the SOI energy (which is the cause of ΔU), that is, $\Delta U = A_{L1}\Delta U_{SOI}$ where A_{L1} is the proportionality constant.

As the LMR measurement is done with a constant current density J_{0L} , the increase in the resistivity by $\Delta\rho$ requires an increase in the measured voltage by ΔV_{Lj} to maintain a constant current density J_{0L} as discussed in §-2. The amount of compensation in the current density is $\Delta J_L = J_{0L} - J_L$ where $J_L = J_{0L} - \Delta J_L = a_{jL}J_{0L}$ is proposed to be the uncompensated current density under the applied external magnetic field.

$\Delta\rho$ carries two changes related to the SOI: (i) the reduction in the energy of the conduction electrons and (ii) the associated reduction in the current density from J_{0L} to J_L by ΔJ_L .

The magnetisation of a ferromagnetic metal sample [32] is given as

$$M = (2M_s/\pi) \times \tan^{-1} \{[(H \pm H_c)/H_c] \tan(\pi M_r/2M_s)\}, \quad (4)$$

where M_s , M_r and H_c are respectively the saturation magnetisation, remanence and coercivity of the ferromagnetic metal sample.

Using eqs (2)–(4), the resistivity of the ferromagnetic metal sample in the LMR measurement can be written as

$$\rho = \rho_0 + \Delta\rho \rightarrow \rho = \rho_0 + \Delta U/(xeJ_L)$$

or using $J_L = a_{jL}J_{0L}$, $\Delta U = A_{L1}\Delta U_{SOI}$ and $\Delta U_{SOI} = \mu_0\mu M/2$,

$$\rho = \rho_0 + [A_{L1}\mu_0\mu M/2]/(xe a_{jL} J_{0L}).$$

Then, using $A_L = A_{L1}/a_{jL}$ and the expression of M

$$\rho = \rho_0 + A_L\mu_0\mu \{[(2M_s/\pi) \times \tan^{-1} \{[(H \pm H_c)/H_c] \tan(\pi M_r/2M_s)\}]/(2xeJ_{0L})\}$$

or using ρ_{HL} for the resistivity of the sample under the external magnetic field \mathbf{H} ,

$$\rho_{HL} = \{\rho_0 + [A_L(\mu_0\mu 2M_s)/(2\pi eJ_{0L}x)] \times \tan^{-1} \{[(H \pm H_c)/H_c] \tan(\pi M_r/2M_s)\}\}. \quad (5)$$

When the lowest resistivity is indicated as ρ_{1L} , the percentage magnetoresistance ratio for the longitudinal measurement is obtained as

$$(\Delta\rho/\rho)_L\% = [(\rho_{HL} - \rho_{1L})/\rho_{1L}] \times 100 \rightarrow (\Delta\rho/\rho)\% = [(\rho_{HL}/\rho_{1L}) - 1] \times 100$$

or

$$(\Delta\rho/\rho)_L\% = \{[(\rho_0 + [A_L(\mu_0\mu M_s)/(\pi eJ_{0L}x)] \times \tan^{-1} \{[(H \pm H_c)/H_c] \tan(\pi M_r/2M_s)\})/(\rho_0 + [A_L(\mu_0\mu M_s)/(\pi eJ_{0L}x)] \times \tan^{-1} \{[(H_{1L} \pm H_c)/H_c] \tan(\pi M_r/2M_s)\})] - 1\} \times 100, \quad (6)$$

where H_{1L} is the value of external magnetic field which gives rise to the lowest resistivity.

2.2 Transverse magnetoresistance measurement in ferromagnetic metals

When an external magnetic field \mathbf{H} is applied perpendicular to the electric current I in the ferromagnetic metal, a net magnetisation \mathbf{M} develops within the ferromagnetic metal perpendicular to the electric current direction as shown in figure 2.

The creation of net magnetisation \mathbf{M} is due to the orientation of the atomic magnetic moments towards the direction parallel to the applied external magnetic field. This orientation of the atomic magnetic moments slightly rearranges the electron cloud about each nucleus due to the SOI as discussed in the section for the LMR geometry and causes a smaller projected cross-sectional area of the electron cloud of the atom to the flow of the conduction electrons. Different values of this projected cross-sectional area for $\mathbf{H}=0$ or $\mathbf{H}\neq 0$ cause different amounts of scattering by the conduction electrons during their passage through the material.

According to the scattering mechanism of Mott's model, the conduction electrons can only scatter into the 3d hole states if the momentum of the conduction electron is in the plane of the classical orbit of the empty d state, which is the case in the LMR geometry. However, as magnetisation \mathbf{M} grows perpendicular to the current density \mathbf{J} in the TMR geometry, the projected cross-sectional area mentioned above is expected to become smaller, and the likelihood of the conduction electron momentum not being in the plane of the classical orbit of the empty d states is expected to increase. This causes a reduction in the probability of s–d scattering and offers less resistance to the conduction electrons [26].

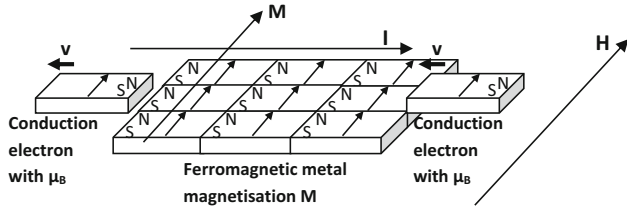


Figure 2. Motion of the conduction electron in the presence of magnetisation in the transverse MR measurement where \mathbf{H} is the applied external magnetic field, I is the applied electric current, v is the velocity, μ_B is the magnetic moment of the conduction electron and \mathbf{M} is the magnetisation of the sample.

Therefore, in the TMR geometry, each conduction electron loses less energy and maintains more energy (or relative increase in its energy) with respect to the case under the initial conditions before the application of the external magnetic field \mathbf{H} . According to the model suggested in this study, the smaller energy loss (relative energy increase) by the conduction electrons along the sample compared to the case under the initial conditions is also proposed to be proportional to the SOI energy of $\Delta U_{SOI} = \mu_0 \mu M / 2$.

From the picture of a good classical imagination, it may be summarised that as a result of the amount of SOI in this geometry, the conduction electrons find themselves encountering less projected cross-sectional area of the electron cloud of the atom in front of them, and therefore less scattering due to SOI with respect to the initial conditions as expected before the application of the external magnetic field \mathbf{H} . The relative energy increase of the conduction electrons in this geometry is expected to give rise to an increase in the current density with respect to the initial conditions before the application of the external magnetic field \mathbf{H} , and eventually a decrease in the resistivity and therefore a change in the variable applied electric voltage is observed as discussed above.

A similar analysis to the one done for the longitudinal measurement for the relation between the initial resistivity ρ_0 and final resistivity ρ (also considering the relation between the initial and final electric current densities J_{0T} and J_T as $J_T = a_{JT} J_{0T}$, where a_{JT} relates J_{0T} to J_T) can be considered for the transverse measurement as follows:

When an external magnetic field \mathbf{H} is applied on the ferromagnetic metal perpendicular to the current direction as shown in figure 2, the value of ρ_0 is expected to change to a smaller value ρ due to (i) the rearrangements of the electron cloud about each nucleus slightly as a result of the SOI, which results in less amount of scattering of the conduction electrons and (ii) the associated relative increase in the electric current density from

J_{0T} to J_T in the ferromagnetic sample in this geometry. The relation between ρ and ρ_0 can therefore be written as

$$\rho = (\rho_0 - \Delta\rho). \quad (7)$$

Here $\Delta\rho = \Delta U / (xeJ_T)$ where $J_T = a_{JT} J_{0T}$ and $\Delta U = (a_{uT} - a_{JT})U_0$ which is related to the changes in the energy U_0 and the current density J_0 by a_{uT} and a_{JT} , and is taken equivalent to $\Delta U = A_{T1} \Delta U_{SOI}$ where A_{T1} is the proportionality constant. The increase in J_{0T} is given as ΔJ_T where $J_T = J_{0T} + \Delta J_T$. The decrease in resistivity $\Delta\rho$ causes a decrease ΔV_j in the measured voltage V to maintain the constant current density J_{0T} .

We use the expressions $\Delta U = A_{T1} \Delta U_{SOI}$, $J_T = a_{JT} J_{0T}$, $U_T = a_{uT} U_0$ (where a_{uT} relates U_T to U_0 and a_{JT} relates J_T to J_{0T}). Following the same procedures as in the analysis of the longitudinal measurement given above, it can be seen that for a positive TMR, $a_{uT} > a_{JT} \rightarrow (a_{uT}/a_{JT}) > 1$, for a negative TMR, $a_{uT} < a_{JT} \rightarrow (a_{uT}/a_{JT}) < 1$ and for zero TMR, $a_{uT} = a_{JT}$. Also, when $A_T = A_{T1}/a_{JT}$, the equation for the resistivity in the transverse measurement can be obtained as

$$\rho_{HT} = \left\{ \rho_0 - \left[\frac{A_T (\mu_0 \mu 2M_s)}{2\pi e J_{0T} x} \right] \times \tan^{-1} \left\{ \left[\frac{(H \pm H_c)}{H_c} \right] \tan(\pi M_r / 2M_s) \right\} \right\}. \quad (8)$$

When ρ_{1T} is the lowest resistivity and ρ_{HT} is the resistivity under the external magnetic field \mathbf{H} , the percentage magnetoresistance ratio for the transverse measurement is obtained as

$$(\Delta\rho/\rho)_T \% = \left[\frac{(\rho_{HT} - \rho_{1T})}{\rho_{1T}} \right] \times 100 \rightarrow (\Delta\rho/\rho)\% = \left[\frac{(\rho_{HT}/\rho_{1T}) - 1}{1} \right] \times 100$$

or

$$(\Delta\rho/\rho)_T \% = \left[\left(\left\{ \rho_0 - \left[\frac{A_T (\mu_0 \mu M_s)}{\pi e J_{0T} x} \right] \times \tan^{-1} \left\{ \left[\frac{(H \pm H_c)}{H_c} \right] \tan(\pi M_r / 2M_s) \right\} \right\} / \left\{ \rho_0 - \left[\frac{A_T (\mu_0 \mu M_s)}{\pi e J_{0T} x} \right] \times \tan^{-1} \left\{ \left[\frac{(H_{1T} \pm H_c)}{H_c} \right] \tan(\pi M_r / 2M_s) \right\} \right\} \right) - 1 \right] \times 100, \quad (9)$$

where H_{1T} is the external magnetic field which gives rise to the lowest resistivity. Because the TMR measurement is done with a constant current density J_{0T} (which is taken as equal to J_{0L}), the decrease in resistivity $\Delta\rho$ requires a decrease in the measured voltage ΔV_{Lj} to maintain a constant current density J_{0T} as discussed in §2. The amount of compensation in the current density is $\Delta J_T = J_{0T} - J_T$ where $J_T = J_{0T} + \Delta J_T = a_{JT} J_{0T}$ is proposed to be the uncompensated current density under the applied external magnetic field.

Table 1. The parameters used in the simulations of eqs (6) and (9). The resistivity values were taken from different studies on similar systems (for CoFe [35], NiFe [36] and Ni [24]) while the magnetic and dimensional data were used from [33,34]. J_L , J_T , ρ_0 , M_s , M_r , H_c , A_L and A_T are defined in the text. x (cm) \times w (cm) \times t (cm) are dimensions of the ferromagnetic metal films.

	ρ_0 (Ω -m)	M_s (A/m)	M_r (A/m)	H_c (A/m)	x (cm) \times w (cm) \times t (cm)	A_L	A_T	$A_L/A_T = J_T/J_L$
CoFe	3.0×10^{-7}	1.597×10^6	0.350×10^6	2.070×10^3	$1 \times 1 \times 2.6 \times 10^{-4}$	1.01	0.69	1.46
NiFe	2.5×10^{-7}	0.779×10^6	0.319×10^6	0.398×10^3	$1 \times 1 \times 3.0 \times 10^{-4}$	1.07	0.93	1.15
Ni	7.8×10^{-8}	0.151×10^6	0.077×10^6	4.770×10^3	$1 \times 1 \times 2.0 \times 10^{-4}$	1.15	0.8	1.44

2.3 Combining longitudinal MR and transverse MR

Using eqs (6) and (9), total MR can be written as

$$(\Delta\rho/\rho)\% = [(\Delta\rho/\rho)_L\%]\cos\theta + [(\Delta\rho/\rho)_T\%]\sin\theta, \quad (10)$$

where θ is the angle between the electric current I and the applied external magnetic field \mathbf{H} .

According to the model presented above, the magnetoresistance ratios given in eqs (6) and (9) depend on the sample's initial resistivity ρ_0 , A_L (for longitudinal MR), A_T (for transverse MR), current density J_L (for longitudinal MR), J_T (for transverse MR), conduction electron magnetic moment μ , sample length x , saturation magnetisation M_s , remanence magnetisation M_r , coercive field H_c and external magnetic field \mathbf{H} . Simulations of these equations are done by varying these parameters to obtain the corresponding longitudinal and transverse MR curves.

3. Results

Expressions for magnetoresistance given in eqs (6) and (9) were tested using the magnetisation and magnetoresistance data taken from [33,34].

The parameters used in the simulations are given in table 1. Because of the difficulty in providing all the parameters from a single source study, the resistivity values given in the table were taken from different studies on similar systems (for CoFe [35], NiFe [36] and Ni [24]) while the magnetic and dimensional data were from [33,34].

Figure 3 shows the simulation curves for the LMR and TMR of the CoFe alloy film studied in [33]. These simulations have been done by varying A_L for the LMR and A_T for the TMR. The ratio between A_L and A_T is $A_L/A_T = 1.46$. In these simulations, the same absolute values of |5.2%| for the LMR with $A_L = 1.01$, |3.6%| for the TMR with $A_L = 0.69$, and almost the same shape of the LMR and TMR curves as in [33] have been obtained. When we take into account the experimental errors in the magnetoresistance measurements in [33], the agreement

between the experimental data in [33] and the corresponding simulation curves in figure 3 is good.

Figure 4 shows another test of the simulation curves for the same CoFe film. In these simulations, the uncompensated current densities J_L and J_T were varied and other parameters were kept constant, assuming $A_{L1} = A_{T1}$. It can be seen in figure 4 that as the uncompensated current density J_L for the LMR and J_T for the TMR becomes bigger, the absolute values of the LMR and TMR get smaller.

The LMR and TMR curves for the same CoFe sample have also been simulated using the mean free path as x (it is assumed to be the sample length) and the cross-sectional area as x^2 (it is assumed to be the cross-sectional area of the sample) instead of the actual dimensions of the sample as shown in figure 5.

As can be seen from figure 5, these two simulations exactly match each other, having different current densities. The uncompensated current density for the simulation using the mean free path value of x is 1.74×10^6 times greater than that for the one using the dimensions of the sample. This difference between the uncompensated current densities in these simulations is due to the change in dimensions while going from the actual dimensions of the sample to the mean free path dimensions under a constant current.

Tests of the magnetoresistance expressions of eqs (6) and (9) have also been done on NiFe alloy film and Ni film. Figures 6 and 7 show the simulation curves for the LMR and TMR effects in the ferromagnetic NiFe film (experimentally studied in figure 3a of [34]) and Ni film, respectively.

The parameters used in the simulations for these films are also given in table 1. The ratio between A_L and A_T for the NiFe film is ~ 1.15 while it is ~ 1.44 for the Ni film.

In these simulations, almost the same shapes and the same absolute maximum values of MRR% as those of the corresponding experimental values of these samples have been obtained (the values of |3.7%| for the LMR and |3.3%| for the TMR curves of the NiFe sample and the values of |3.4%| for the LMR and |2.2%| for the TMR curves of the Ni sample). When we take

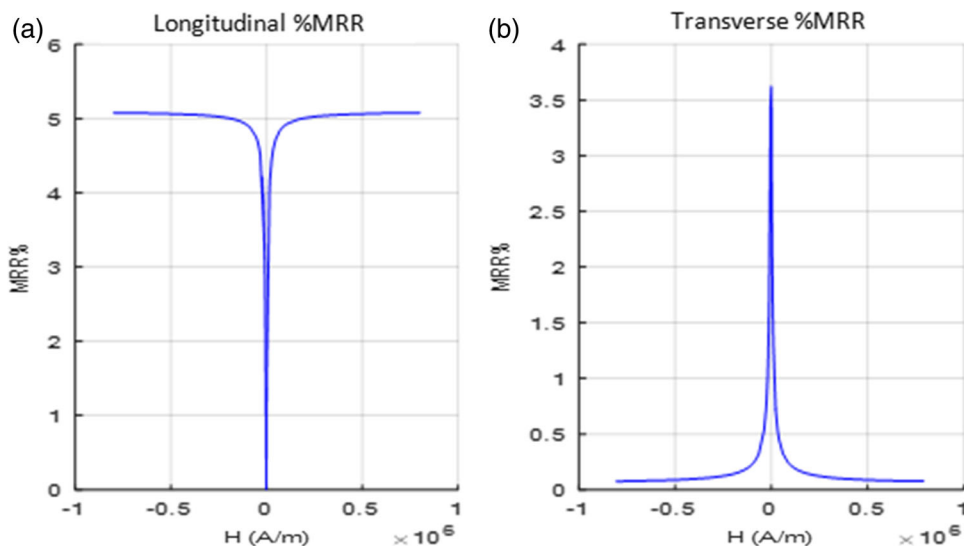


Figure 3. The simulation curves for (a) LMR using eq. (6) and (b) TMR using eq. (9) for the CoFe alloy film in figure 3 of [33].

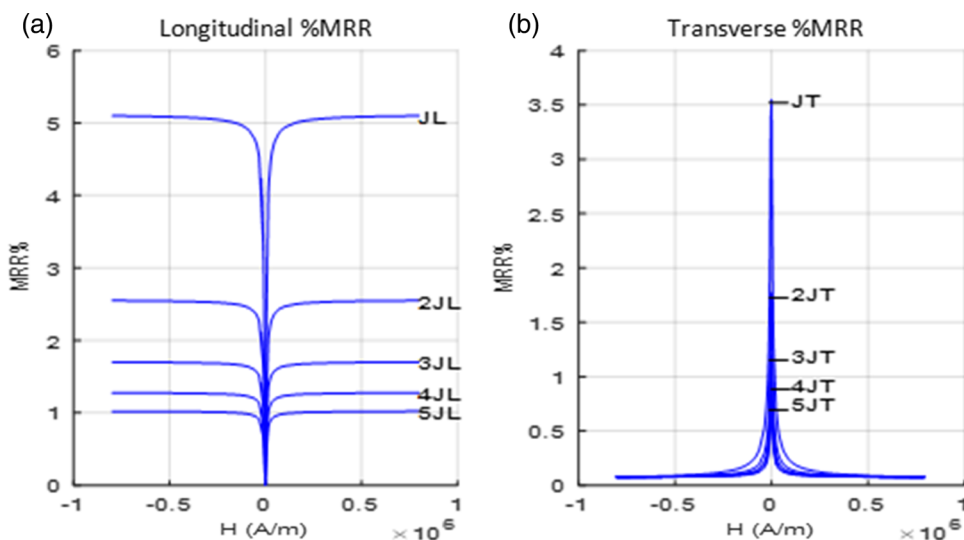


Figure 4. The simulations of the magnetoresistance curve of eqs (6) and (9) for (a) the LMR curve and (b) the TMR curve of the CoFe film as a function of uncompensated electric current density. $J_L, 2J_L, 3J_L \dots$, and $J_T, 2J_T, 3J_T \dots$, indicate the positions of the maximum values of LMR and TMR for the corresponding uncompensated electric current densities.

into account the experimental errors in the magnetoresistance measurements, the agreement between the experimental data of these samples and the corresponding simulation curves in figures 6 and 7 are also good.

4. Discussions

According to the model described above, the positive increase in the LMR of the samples mentioned above is due to the relative decrease in the energies of the conduction electrons (by ΔU) associated with a decrease in the electric current densities because of more scattering

interactions with respect to the case when an external magnetic field is not applied. These decreases are compensated by the voltage increase to maintain a constant current. The negative increase in the TMR of these samples is due to the relative increase in the energies of the conduction electrons (by ΔU) associated with an increase in the electric current densities because of fewer scattering interactions with respect to the case when an external magnetic field is not applied. These increases are compensated by the decrease in voltage to maintain again a constant current.

The defined parameters A_L for the LMR and A_T for the TMR are proposed to be representing the ratio

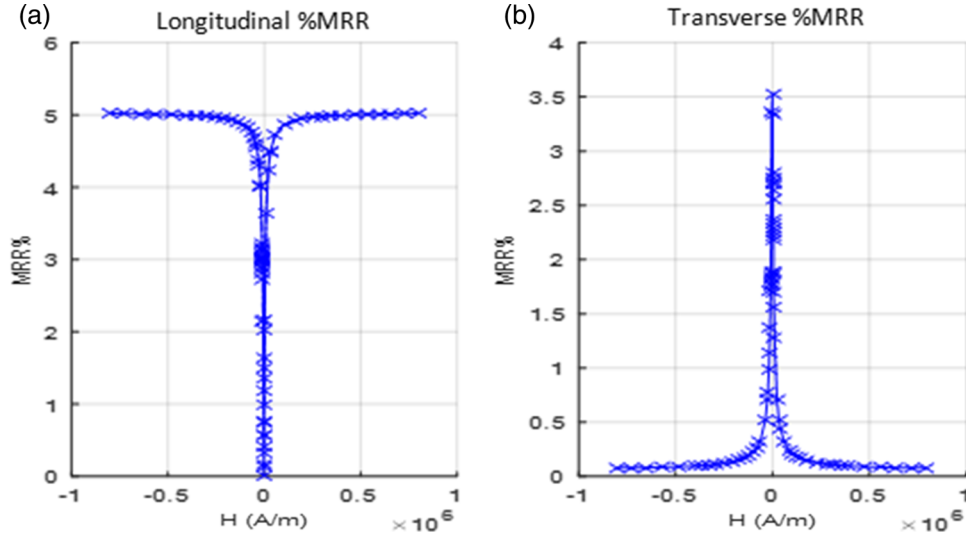


Figure 5. (a) The LMR data and (b) the TMR data simulated using the dimensions of the sample (crosses), and using the mean free path (x) and the cross-sectional area (x^2) (solid lines).

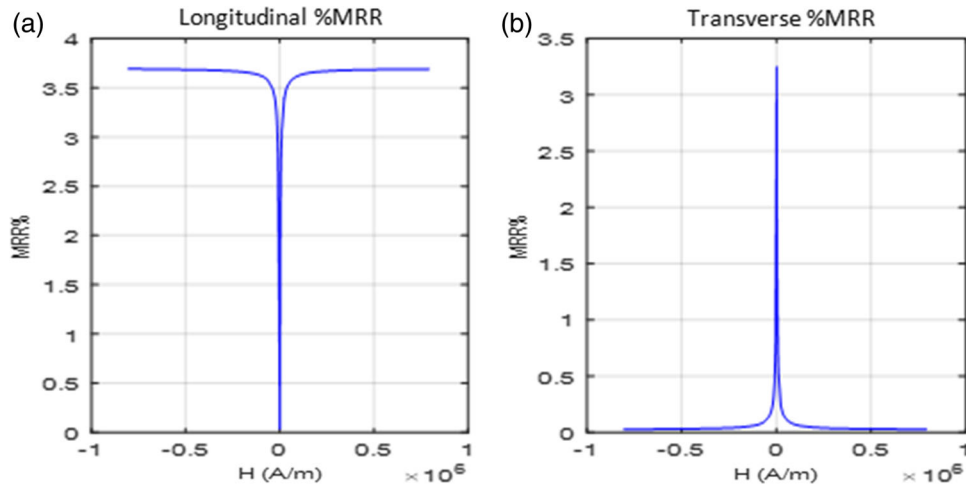


Figure 6. The simulations for the magnetoresistance curves of NiFe film. The curves represent the simulations for (a) the LMR using eq. (6) and (b) the TMR using eq. (9).

between the change in the energy of conduction electron per SOI energy (defined by $A_{L1} = \Delta U / \Delta U_{SOI}$ for the LMR and $A_{T1} = \Delta U / \Delta U_{SOI}$ for the TMR) and the relative amount of uncompensated current density (defined by $a_{JL} = J_L / J_{0L}$ for the LMR and $a_{JT} = J_T / J_{0T}$ for the TMR). The ranges of the values of A_L and A_T for the CoFe, NiFe and Ni metal films can be obtained from table 1 as $1.0 < A_L < 1.2$ and $0.6 < A_T < 1.0$.

If we assume that $|\Delta U| = |A_{L1} \Delta U_{SOI}|$ for the LMR measurement is equal to $|\Delta U| = |A_{T1} \Delta U_{SOI}|$ for the TMR measurement (that is, $\Delta U = A_{L1} \Delta U_{SOI} = A_{T1} \Delta U_{SOI}$ with ΔU_{SOI} which is the same for the LMR and TMR measurements, then $A_{L1} = A_{T1}$), the magnitudes of J_L and J_T (where $J_L = a_{JL} J_{0L}$ and $J_T = a_{JT} J_{0T}$ with $J_{0L} = J_{0T}$ and $a_{JT} > a_{JL}$) are expected

to affect the magnitude of magnetoresistance, that is, a bigger uncompensated current density gives rise to less magnetoresistance effect as can be seen from the equation $|\Delta \rho| = |\Delta U| / (xeJ_{L,T})$. Upon this assumption, using $A_{L1} = A_{T1}$, and having J_T ($J_T = J_{0T} + \Delta J_T = a_{JT} J_{0T}$) greater than J_L ($J_L = J_{0L} - \Delta J_L = a_{JL} J_{0L}$) because $a_{JT} > a_{JL}$, the difference between the absolute values of the longitudinal and transverse magnetoresistance is attributed to the uncompensated current density difference between J_T and J_L in these measurements. This means that a bigger uncompensated current density gives rise to a smaller magnetoresistance with the relative rearrangements of the electron clouds about each nucleus due to the SOI interaction as discussed in §2.1 and 2.2 for the LMR and TMR geometries.

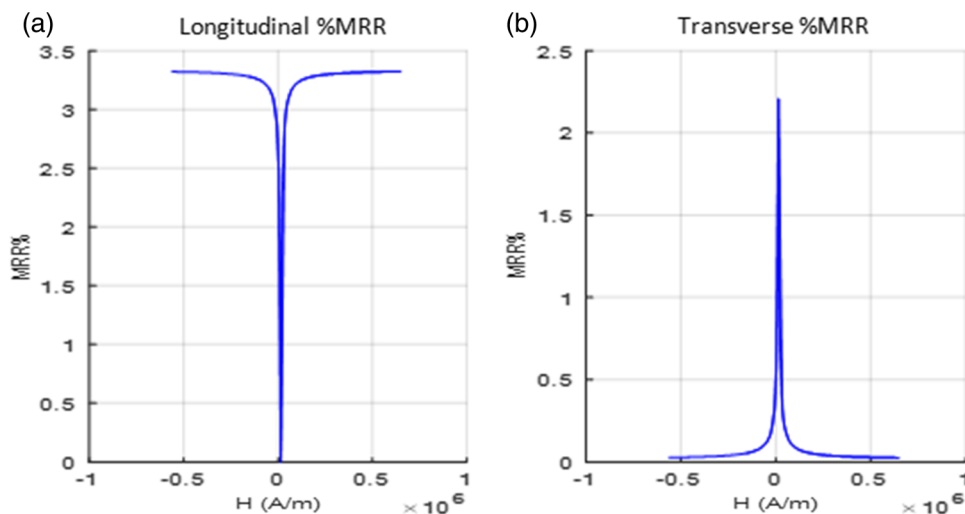


Figure 7. The simulations of magnetoresistance curves of Ni film. The curves represent the simulations for (a) the LMR using eq. (6) and (b) the TMR using eq. (9).

Therefore, the difference between the absolute maximum value of LMR and the absolute maximum value of TMR for the CoFe, NiFe and Ni films is attributed to the uncompensated current density difference between J_T and J_L due to the relative rearrangements of the electron clouds about each nucleus as a result of the SOI in these measurements.

The expressions (eqs (6) and (9)) obtained in this study relates the resistivity of a sample under an applied external magnetic field to the parameters A_L or A_T , initial resistivity ρ_0 , current density, conduction electron magnetic moment μ , sample length, saturation magnetisation M_s , remanence magnetisation M_r , coercive field H_c and external magnetic field \mathbf{H} . Therefore, our model predicts that when an external magnetic field is applied to a ferromagnetic metal sample, the energy of the conduction electron and therefore the current density are affected causing a change in resistivity (magnetoresistance) as a function of these parameters. To predict the exact magnitude and shape of the magnetoresistance curve, we must know the parameters in these equations. Any change in these parameters may strongly affect the magnetoresistance curve and give very different shapes and magnitudes.

5. Conclusions

In this study, an attempt is made to develop a model to analyse the anisotropic magnetoresistance in ferromagnetic metal samples. In the model described in this study, the change in the energy of conduction electron, ΔU , upon the application of an external magnetic field

as it flows through the ferromagnetic sample is proposed to be proportional to the amount of SOI energy, $\Delta U_{SOI} = \mu_0 \mu M / 2$. This idea has been used to develop eqs (6) and (9) relating the resistivity of a sample under an applied external magnetic field to the parameters A_L or A_T , initial resistivity ρ_0 , current density, conduction electron magnetic moment μ , sample length, saturation magnetisation M_s , remanence magnetisation M_r , coercive field H_c and external magnetic field \mathbf{H} .

As described in §4, by fitting eq. (6) to the experimental data of LMR measurements (or fitting eq. (9) to those of TMR measurements), the value of A_L (or A_T), that is, the change in the energy of conduction electron per SOI energy and the relative amount of uncompensated current density can be determined. In this study, the values of A_L and A_T for the CoFe, NiFe and Ni metal films (see table 1) have been determined to be within the ranges of $1.0 < A_L < 1.2$ and $0.6 < A_T < 1.0$.

Assuming $A_{L1} = A_{T1}$ for the longitudinal and transverse measurements, it is also determined that as the uncompensated current density becomes bigger, the LMR and TMR values get smaller (see figure 4). Assuming that $A_{L1} = A_{T1}$, the difference between the absolute values of the LMR and TMR is related to the uncompensated current density difference ($J_T - J_L$) due to the relative rearrangements of the electron clouds about each nucleus due to the SOI interaction.

The LMR and TMR curves for the samples mentioned above have been simulated using the macroscopic dimensions of the sample. They have also been simulated using the mean free path x and the cross-sectional area x^2 . With a difference in the uncompensated electric current densities due to the dimensional difference

in these simulations, both simulations have fitted well to the experimental anisotropic magnetoresistance data of the ferromagnetic metal films.

Considering the experimental errors, although good agreements between the experimental curves and the corresponding simulation curves for the samples given in table 1 were obtained, additional experimental AMR curves with enough and accurate data of similar other ferromagnetic systems are needed for further justification of these equations (eqs (6) and (9)).

However, to our knowledge, these equations (eqs (6) and (9), which are composed of measurable physical parameters, obtained in a much simpler way than most of those present in the literature, simulate the experimental data very well and may be seen as another proof of the validity of the SOI used to explain AMR effect) are the first equations to be derived in the manner discussed above using Ohm's law and the spin-orbit interaction.

Acknowledgements

The author would like to thank Dr Michael F Thomas for his extensive comments and discussions on the microscopic mechanisms of magnetoresistance and also Prof. Dr Mürsel Alper for providing the data of Ni films.

References

- [1] J Daughton, J Brown, E Chen, R Beech, A Pohm and W Kude, *IEEE Trans. Magn.* **30(6)**, 4608 (1994)
- [2] V Lemarquand and G Lemarquand, *IEEE Trans. Magn.* **31(6)**, 3188 (1995)
- [3] K Mohri, T Uchiyama and L V Panina, *Sensors Actuators A* **59**, 1 (1997)
- [4] M I Piso, *J. Magn. Magn. Mater.* **201**, 380 (1999)
- [5] G R Pattanaik, D K Pandya and S C Kashyap, *J. Electrochem. Soc.* **149(7)**, C363 (2002)
- [6] M Pasquale, *J. Magn.* **8(1)**, 60 (2003)
- [7] J Lenz and A S Edelstein, *IEEE Sens. J.* **6(3)**, 631 (2006)
- [8] M Bedir, Ö F Bakkaloğlu, I H Karahan and M Öztaş, *Pramana – J. Phys.* **66(6)**, 1093 (2006)
- [9] I H Karahan, Ö F Bakkaloğlu and M Bedir, *Pramana – J. Phys.* **68(1)**, 83 (2007)
- [10] M Hassan, A Zeeshan, A Majeed and R Ellahi, *J. Magn. Magn. Mater.* **443**, 36 (2017)
- [11] M M Bhatti, A Zeeshan and R Ellahi, *Pramana – J. Phys.* **89**, 48 (2017)
- [12] A Zeeshan, A Majeed, R Ellahi and Q M Z Zia, *Therm. Sci. J.* **22(6)**, 2515 (2018)
- [13] A Majeed, A Zeeshan, S Z Alamri and R Ellahi, *Neural. Comput. Appl.* **30(6)**, 1947 (2018)
- [14] M Sheikholeslami, R Ellahi, A Shafee and Z Li, *Int. J. Num. Met. for Heat and Fluid Flow* **29(3)**, 1079 (2019)
- [15] A Sohail, M Fatima, R Ellahi and K B Akram, *J. Mol. Liq.* **285**, 47 (2019)
- [16] Y Mohammadmoradi and M Yaghobi, *Pramana – J. Phys.* **93(2)**, 25 (2019)
- [17] M R Niazzian, L F Matin, M Yaghobi and A A Masoudi, *Indian J. Phys.* **95(6)**, 1131 (2021)
- [18] S Kokado, M Tsunoda, K Harigaya and A Sakuma, *J. Phys. Soc. Jpn.* **81**, 024705 (2012)
- [19] I Campbell, A Fert and O Jaoul, *J. Phys. C: Solid State Phys.* **3**, S95 (1970)
- [20] A Malozemoff, *Phys. Rev. B* **32**, 6080 (1985)
- [21] M Tsunoda, H Takahashi, S Kokado, Y Komasaki, A Sakuma and M Takahashi, *Appl. Phys. Exp.* **3(11)**, 113003 (2010)
- [22] C Rizal and B B Niraula, *J. Nano-Electron. Phys.* **7(4)**, 04068 (2015)
- [23] T Kasuya, *Prog. Theor. Phys.* **16(1)**, 58 (1956)
- [24] T R McGuire and R I Potter, *IEEE Trans. Magn.* **11(4)**, 1018 (1975)
- [25] I Bakonyi and L Peter, *Prog. Mater. Sci.* **55(3)**, 107 (2010)
- [26] R C O'Handley, *Modern magnetic materials: Principles and applications* (John Wiley & Sons, New York, USA, 2000) p. 86, 580
- [27] N F Mott, *Proc. R. Soc. A* **153(880)**, 699 (1936)
- [28] A Fert and I A Campbell, *Phys. Rev. Lett.* **21(16)**, 1190 (1968)
- [29] F Gautier and B Loegel, *Solid-State Commun.* **11(9)**, 1205 (1972)
- [30] J W F Dorleijn and A R Miedema, *J. Phys. F: Met. Phys.* **7(1)**, L23 (1977)
- [31] B D Cullity and C D Graham, *Introduction to magnetic materials* (John Wiley & Sons, New Jersey, USA, 2009) p. 272
- [32] S Honda, T Okada and M Nawate, *J. Magn. Magn. Mater.* **165(1–3)**, 326 (1997)
- [33] H Kockar, M Alper, T Sahin and O Karaagac, *J. Magn. Magn. Mater.* **322(9–12)**, 1095 (2010)
- [34] H Kuru, H Kockar, M Alper and O Karaagac, *J. Magn. Magn. Mater.* **377**, 59 (2015)
- [35] S Mehrizi and M H Sohi, *J. Mater. Sci. Mater. Electron.* **26(10)**, 7381 (2015)
- [36] K A Deepthi, R Balachandran, B H Ong, K B Tan, H Y Wong, H K Yow and S Srimala, *Appl. Surf. Sci.* **360(Part B)**, 519 (2016)